

SMART WHEEL-BASED STAIR-CLIMBING ROBOT

B. Strah, S. Rinderknecht

Institute for Mechatronic Systems in Mechanical Engineering, Technische Universität Darmstadt
Otto-Berndt-Straße 2, 64287 Darmstadt, Germany
{strah,rinderknecht}@ims.tu-darmstadt.de

Key words: Wheel-based stair-climbing robot, Hybrid nonlinear dynamics, Unilateral contacts, Underactuation, Feedback linearization, Virtual constraints.

Summary: *Smart aspects in development of a wheel-based robot which is capable to climb stairs autonomously are presented. Autonomy connotes the ability to climb stairs without any mechanical contact to environment except ground contact with wheels. A comparison of wheel-based to other known locomotion systems is given. Advantages of wheel-based systems are emphasized. The presented Stair Climber (SC) robot uses a rotated chassis whereat the number of contacts between wheel pairs and ground alternates between one and two. As consequence, the SC experiences discontinuous dynamics due to wheel-to-ground repeating contact activations and deactivations. Moreover, the continuous dynamics characteristics of the SC distinguish in different contact situations. Consequently, the SC model is of hybrid dynamics. Methodic aspects of the research and development of the SC are given in overview focusing on modeling and control design. The control design contains a strategy for stair-climbing which is realized as a sequence of different motion types. These motion types include motion along equilibrium points as well as motion in between equilibrium points crossing discrete state borders. Since the system is of nonlinear dynamics, feedback linearization techniques are applied. Specific for one of the SC states is underactuation which has to be considered in control design. Furthermore, one state transition is realized within the virtual constraints framework resulting in smooth wheel-to-ground contact activations. Typical results cover the presented SC. Development perspectives of existing SC are given.*

1 INTRODUCTION

A wheel-based locomotion principle capable to climb stairs autonomously, which is implemented within a robot prototype, is presented. Autonomy addresses the ability to climb stairs without any physical contact with the robot's environment, except wheel-to-ground contact.

After a motivation and state-of-the-art consideration from application and methodological point of view, the main chapters give only an overview over the development process. While concrete description regards to the existing *Stair Climber* robot (SC, Figure 2) representing the major part, a further development perspective of a new robot (denoted SC₂, Figure 3) is commented at some points.

1.1 Motivation

Communication ability, information exchange, goods transportation and mobility of human are important factors of human society. They influence both professional and personal areas of life, providing prosperity and enhancing the quality of life, especially considering ageing society. Everyday situations in our urban environment are embossed by spending time and effort mastering these issues, even for simplest tasks.

Most obviously, even a single stair like curb or doorstep can present the mobility border for a wheelchair driver or a simple wheel-based robot. Possibilities to overcome such borders are either development of different locomotion principles or extensive infrastructure extension like ramp access, elevator or transporting mechanisms.

While in industrial and professional environment infrastructure measures often are designed in advance allowing reaching important locations physically, a communication infrastructure allowing robotized vehicles navigation ability is less available. Reaching the goal location including the “last mile” in some smaller or older professional environment as well as historic, touristic and domestic environment remains challenging. The reasons for non-existent infrastructure can be complex, considering historical, financial and architecture design aspects.

On the other hand, there exist different locomotion principles (commercially available or still in research) capable of (potentially) reaching the goal in a human-centered environment. The locomotion principle of the robot treated here has some advantages from commercial point of view. To mention briefly, dynamics, comfort, energy efficiency, movability, complexity of mechanical setup and acceptance in domestic environment are addressed.

Since human-centered urban environment consists mostly of flat surfaces connected through staircase or stairs, a robot intended to interact with human should have the ability of stair-climbing.

Autonomy in stair-climbing, which is a must in case of wheel-based robots and welcomed in general for wheel-based vehicles, is a demanding task. It includes robot environment perception and navigation ability and specific locomotion ability. The specific locomotion ability is addressed here, demonstrating it in a wheel-based autonomous stair-climbing robot.

Seen as general mobile platform, this robot can be used as basis for further development of different applications. Possible are applications in domain of personal transportation, especially wheelchairs for mobility-impaired [1], tele-presence robots and logistics as well as transportation addressing last mile delivering, to mention only a few.

1.2 Locomotion principles considering motion in structured environment

Considering motion in human-centered urban environment which is often well structured, different locomotion principles are possible. The aim here is not to give a detailed register of all possible principles and variations, but rather the most common locomotion principles which for one or another reason are in use or in research.

Basically, different locomotion principles, like wheel-based, leg-based, crawlers or hybrid (e.g. combination of wheels and legs) are known. In typical everyday locomotion situations, consisting mostly of motion along flat ground, wheel-based systems compared to leg-based or crawlers have advantages of a relatively low energy consumption, high motion velocity [2] [3] [4] and high movability. An advantage of robot principle here comparing to crawlers and some other wheel-based principles could be the home acceptance, since in normal operation it does not slip over the leading edge. Therefore, the staircase remains free from damage or mechanical signs of usage. An advantage over the leg-based locomotion systems and some

other systems is a relatively light and simple construction. This can be crucial for the mass-market acceptance.

Hence, wheel-based systems have some advantages but comparing to previous mentioned locomotion systems, the simple wheel-based systems are not appropriate for motion in unstructured environment like in disaster situations or for climbing stairs. Examples are commercially available products like the individual transporter *Segway* and telepresence robot *Double* (www.doublerobotics.com). The crucial disadvantage in usual everyday situations for structured environment including home environment is the inability of stair-climbing. The capability of stair-climbing by retaining the previous wheel-based system advantages and functionality enhancement is the main issue of the presented locomotion principle.

A wheel-based system mechanically similar to the robot considered here is the stair-climbing wheelchair *iBOT* [5]. When climbing stairs it requires an outer force action when shifting the center of gravity [5] [6]. This is not needed at presented robot. Therefore it provides full autonomy at climbing stairs without handrails and allows to climb stairs for people with high degree of disability or unmanned robots.

A further wheel-based robot capable to climb a single step autonomously is presented in a series of publications [7] [8] [9]. The state transitions are handled according to certain specifications. For instance, during settling on the step a soft landing is sought. Both, vertical touchdown velocity of the front wheels and the longitudinal path of the rear wheels are considered for zeroing during the settling. With the applied methodology, this objective can theoretically be achieved only approximately. Since this robot cannot climb steps with short tread compared to wheelbase, the development goes towards two-legged robot with wheels [3] [10]. However, the elimination of this disadvantage succeeds at the cost of considerably more complex mechanism.

An autonomous hybrid two-legged robot with additional wheels capable of climbing a step with possibility to transport a person is described in [4]. With an even more complex mechanism, this robot has the possibility to move on flat surfaces using wheels, while stair-climbing is performed on feet. For operational reasons, lateral-tilting movements during stair-climbing also affect the dynamics, which is not desirable.

1.3 Methods

The methodological treatment of hybrid dynamic systems (HDS) such as modeling is known [11] [12] but the subject topics that are ubiquitous in the field of continuous systems such as the theoretical analysis of stability seems impossible [12]. The modeling of mechanical systems with unilateral contacts is described e.g. in [13] and [14]. A simulation practice of such systems, which are considered as hybrid dynamic systems is a challenge due to their complexity and the numerical robustness and is the subject of research [15] [16] [17].

The control of hybrid dynamic systems is more complex than that of continuous systems, because in addition to the continuous state vector, the interaction with the discrete state needs to be considered. Control methods are only available for specific classes of HDS [12]. Thus model predictive control is developed e.g. for piecewise linear systems.

Methods considering nonlinear hybrid dynamical systems with underactuation and unilateral contacts such as *SC* were primarily developed for two-legged robots (e.g. [18] [19]). The issue mainly refers to the gait, which is designed as a stable limit cycle in hybrid sense. These methods are based on (partial) feedback linearization [20] involving virtual constraints between certain degrees of freedom (DOF). The virtual constraints are defined as

output functions within feedback linearization design procedure. As a result, stable limit cycles occur, which represent the system gait. Obtaining equilibrium (e.g. a standing on a point-foot robot) is considered less.

The transition of a system to an equilibrium and/or its preserving was the research topic of some simpler mechanical systems representing double inverted pendulum (wheel-based "WAcrobot" [21] or fixed to ground "Acrobot" [22] [23]). They consist only of continuous-time dynamics but still obtain underactuation. The control for preserving the upper equilibrium position was either directly realized [21] [22] or after a partial feedback linearization [23]. The transition to the upper equilibrium position at the "Acrobot" is performed by swinging based on a partial feedback linearization and then switched to the mentioned controller for equilibrium preserving.

2 SYSTEM DEVELOPMENT

To meet the requirements of motion on flat ground and stair-climbing ability a locomotion mechanism shown in Figure 1 was considered. Addressed are energy-efficiency, mechanical setup simplicity, motion dynamics, comfort, mobility and acceptance for domestic environment (tall, human-centered applications robot for motion in narrow spaces).

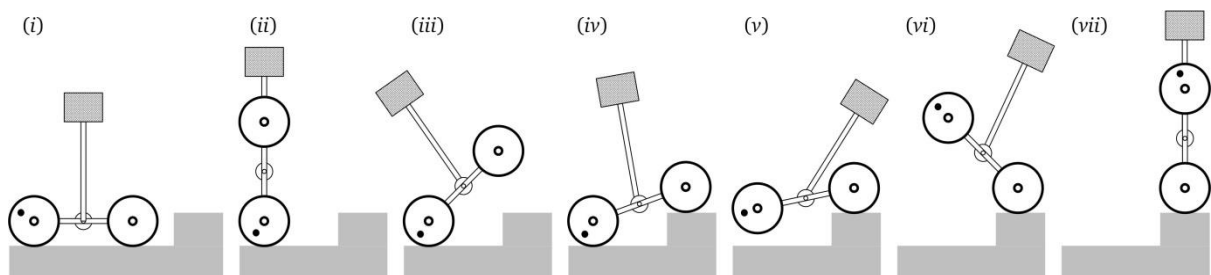


Figure 1: Sketch of the robot at different situations ((i) to (vii)) which demonstrate a sequence of positions during stair-climbing procedure.

The mechanism of the built robot [24], named *SC (Stair Climber)*, consists of driven wheels connected on the lower body (chassis) which itself is capable of rotation about an upper body (Figure 2). The rotation of the chassis is theoretically designed to allow infinite number of rotation. Current status of prototype allows only one turn due to electrical cables for motors and sensors. However, a different component topology could allow infinite number of rotation.

During normal operation mode two possible discrete states are in use. First, it is possible that the system is with both wheel pairs in contact to ground (state S_3), Figure 1-*i*. Second, only one wheel pair can be in contact to ground (state S_1), Figure 1-*ii*. These two states can interchange.

Only rear wheels (denoted by a dot in Figure 1) are driven in current prototype. Hence, in practice only a half rotation of the chassis was applied. Nevertheless, this was enough to prove the concept due to symmetry regarding the chassis rotation axis.

For all drives 150 W DC-Motors were used in current control operation mode. For rear wheels the drives were equipped with planetary gears using a gear reduction of 21. The chassis rotation drives (upper body drives) were equipped with harmonic drives and a gear reduction of 100. Both upper body drives were driven synchronously considering higher-frequency torsional bending mode of upper body.

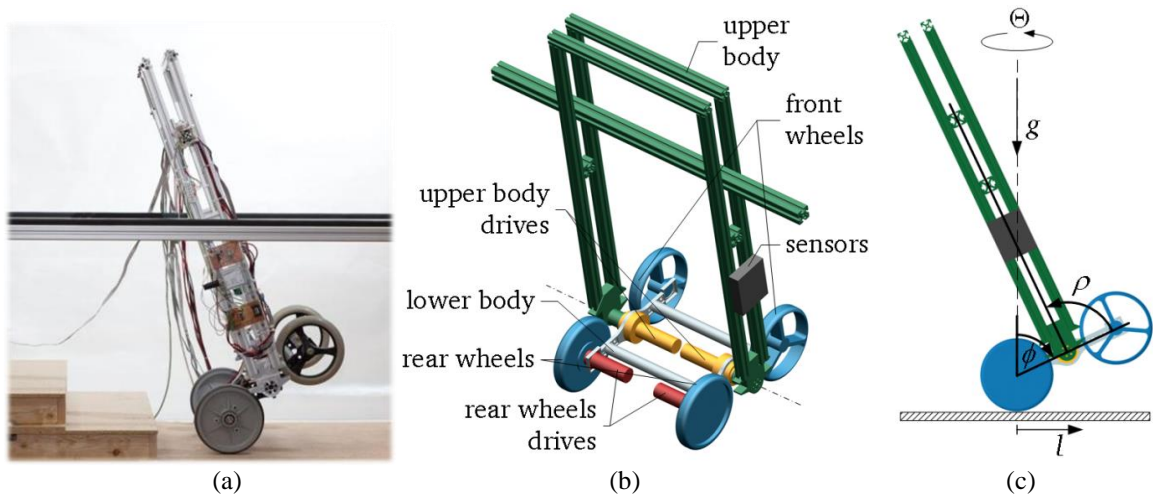


Figure 2: (a) Robot *SC*; (b) CAD-model showing main parts; (c) main DOFs: longitudinal position l , inclination angle ϕ , relative angle between upper and lower body ρ , yawing angle Θ .

All drives have integrated incremental sensors to get the relative angle and angle velocity information. For an precise determination of the inclination angle ϕ , which is crucial for stabilization, data from two sensors, a gyroscope and a inclinometer are fused.

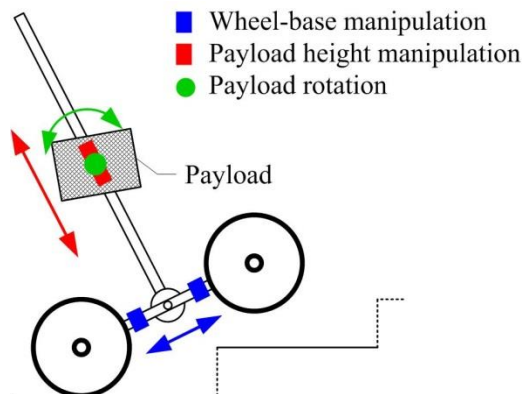


Figure 3: Sketch of a new robot, *SC*₂.

The *SC* was controlled using the dSPACE real-time system. The control algorithms were developed partly in Mathematica and partly in Matlab and implemented into the dSPACE environment.

Functional requirements on different kind of motion are defined at the beginning. The concept of motion can be reduced to following main motion modes relating to DOFs defined in Figure 2-c:

- motion along longitudinal direction l and yawing around Θ , with simultaneous upper body adjustment around ρ in two discrete states, S_1 and S_3 ,
- state transitions relating the number of wheel pairs in ground contact:
 - state transition *settling* ($S_1 \rightarrow S_3$, e.g. Figure 1, situation (iii) to situation (iv))
 - state transition *lift-off* ($S_3 \rightarrow S_1$, e.g. Figure 1, situation (iv) to situation (iii)).

The state transitions are induced by dynamical action of system bodies – there is no additional mechanism with mechanical contact to *SC* environment. Hence, autonomous stair-

climbing with no external support is fulfilled.

Stair-climbing can be achieved by applying a reasonable sequence strategy of mentioned motion modes. It is exemplarily sketched in Figure 1.

A further development of the existing SC could give enhanced functionality. For this new robot (SC_2 , Figure 3) additional DOFs are thinkable. A variable wheel-base would allow more flexibility regarding different stair geometry. Payload manipulation would increase the applicability. Although all DOFs can be included into the control design, it is expected that the payload height manipulation has the most influence to shape the overall dynamics. The practical aspect of payload rotation is to increase comfort during transportation by holding an constant orientation angle.

3 MODELING AND SIMULATION

A model was developed for system analysis as well as for model-based control methods. Functionally, the system dynamics consists of an interaction of both continuous-time and discontinuous behavior. Hence, a hybrid dynamic model of the robot was necessary. While the theoretical principles are known, the implementation for the simulation with objective of high efficiency and numerical robustness represents a challenge. An overview with additional explanation is given in following, while more mathematical details are available in [24] [25].

Considering new development of the SC_2 , changes to SC are expected in continuous-time part of the model.

3.1 Hybrid dynamic model

The hybrid dynamic model is represented in Figure 4 as a hybrid automaton. Four discrete states are considered based on possible wheel-to-ground contact situations:

- State S_0 – *no wheel pair in ground contact*,
- State S_1 – *rear wheel pair in ground contact*,
- State S_2 – *front wheel pair in ground contact*,
- State S_3 – *both wheel pairs in ground contact*.

While in normal operation only states S_1 and S_3 are enough to be considered, states S_2 and S_0 are added to complete the set of possible contact situations. The state S_2 can be considered as symmetric case to S_1 since rear and front wheel pair can switch the meaning. The state S_0 can occur in two situations. First, if due to a bigger disturbance the robot falls down to the lower step. Second, if a high-dynamic action coming out from actuators causes a jump. Therefore, keeping the state S_0 in consideration is useful to represent and prevent these unwanted situations.

In general, state transitions depend on guard functions \mathcal{G} defining the conditions which have to be fulfilled to allow state transition.

Exemplarily, the event causing *lift-off* ($S_3 \rightarrow S_1$) of front wheels is the contact deactivation $\mathcal{C}_{E,f}$ which happens when the wheel-to-ground contact force becomes zero. This contact force ability is denoted as unilateral constraint. Hence, the associated guard function $\mathcal{G}_{3 \rightarrow 1}$ depends only on one condition:

$$\mathcal{G}_{3 \rightarrow 1} := \mathcal{C}_{E,f}. \quad (1)$$

The event causing *settling* ($S_1 \rightarrow S_3$) is contact activation $\mathcal{C}_{A,rf}$, which happens when the front wheel pair distance to ground becomes zero and touchdown velocity $J_{A,f}$ becomes zero.

Therefore, the appropriate guard function is defined as:

$$\mathcal{G}_{1 \rightarrow 3} := J_{A,f} \wedge \mathcal{C}_{A,r,f}. \quad (2)$$

If a touchdown with front wheel pair happens with velocity bigger than zero ($J_{A,f}$) and a rebound $J_{E,f}$ is caused, then the state S_1 is preserved ($S_1 \rightarrow S_1$). The guard function follows as:

$$\mathcal{G}_{1 \rightarrow 1} := J_{A,f} \wedge J_{E,f}. \quad (3)$$

This situation unfortunately can repeat and is known as *Zeno*-behavior.

At state transitions the continuous system state vector is reset in certain cases by function \mathcal{R} .

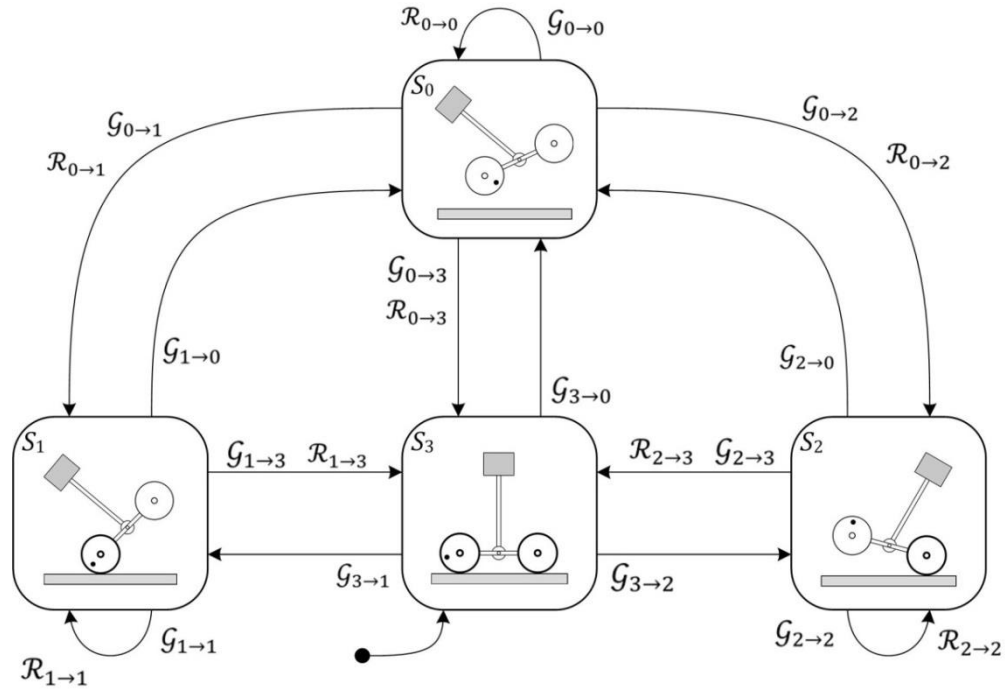


Figure 4: Hybrid dynamic model of the SC represented as hybrid automaton.

Concretely, considering contact activation events, the ground normal direction velocity of the wheels is set to zero ($\mathcal{R}_{1 \rightarrow 3}$). In cases where a wheel rebound occurs, the ground normal direction velocity of the wheels changes its sign ($\mathcal{R}_{1 \rightarrow 1}$).

3.2 Continuous-time dynamics

For each discrete state S_i , $i = \{0,1,2,3\}$, a continuous model was derived using Lagrange's equations of the 1st kind. This systematic modelling procedure includes kinematical constraints giving information on both system dynamics and constraint force components.

The procedure starts with the SC's geometry description (Figure 5-a). System relevant coordinate systems are denoted with a – absolute coordinate system and b – coordinate system on axle of rear wheels. System relevant points are at center of left (l) and right (r) wheel respectively. Main geometry parameters are: distance between point b and lower body COG, $L = 0.15$ m; distance between rotation axle and upper body COG, $H = 0.47$ m; wheel radius $R = 0.1$ m and half-track width $B_w = 0.2$ m.

All considered DOFs are collected in the system dependent coordinates \mathbf{q} :

$$\mathbf{q} = [{}^a x_b, {}^a y_b, {}^a z_b, \alpha_{l,b}, \alpha_{r,b}, \phi, \rho]^T. \quad (4)$$

Additionally introduced particular coordinates ${}^a x_b$, ${}^a y_b$ and ${}^a z_b$ represent the position of the lower body COG regarding absolute coordinate system and the angle of the rear left $\alpha_{l,b}$ and right $\alpha_{r,b}$ wheel respectively. Relatively light front wheels are not considered for rotation, since they are not driven in current state of the robot.

The next step in modeling procedure is definition of the kinematic constraints. Due to stair-climbing functionality, considered are wheel-to-ground kinematic constraints. They differ in each of the discrete states S_i . Correspondingly, the kinematic constraints are defined in form of a matrix equation on velocity level, since some of them are non-holonomic:

$$\Phi_{\mathbf{q},S_i} \dot{\mathbf{q}} = \mathbf{0}. \quad (5)$$

The kinematic constraint matrix $\Phi_{\mathbf{q},S_3}$ for state S_3 includes the constraints which prevent penetration of both wheel pairs into the ground, as well as both lateral and longitudinal sliding of rear wheel pair. It was derived in [24] as:

$$\Phi_{\mathbf{q},S_3}(\mathbf{q}) = \begin{bmatrix} -2 \cos \Theta & -2 \sin \Theta & 0 & R & R & 2R & 0 \\ \sin \Theta & -\cos \Theta & 0 & 0 & 0 & 0 & 0 \\ 0 & 0 & 1 & 0 & 0 & 0 & 0 \\ 0 & 0 & 1 & 0 & 0 & -2L \sin \phi & 0 \end{bmatrix}. \quad (6)$$

Discrete states S_1 and S_2 face less kinematic constraints due to single pair wheel-to-ground contacts. Hence, kinematic constraint matrices consist of fewer rows. The matrix $\Phi_{\mathbf{q},S_1}$ consist of first three rows of $\Phi_{\mathbf{q},S_3}$ relating to constraints of rear wheel pair. The matrix $\Phi_{\mathbf{q},S_2}$ consist of last row of $\Phi_{\mathbf{q},S_3}$ relating to constraint of front wheel pair. Finally, the matrix $\Phi_{\mathbf{q},S_0}$ is a void matrix since the state S_0 is free from wheel-to-ground contacts.

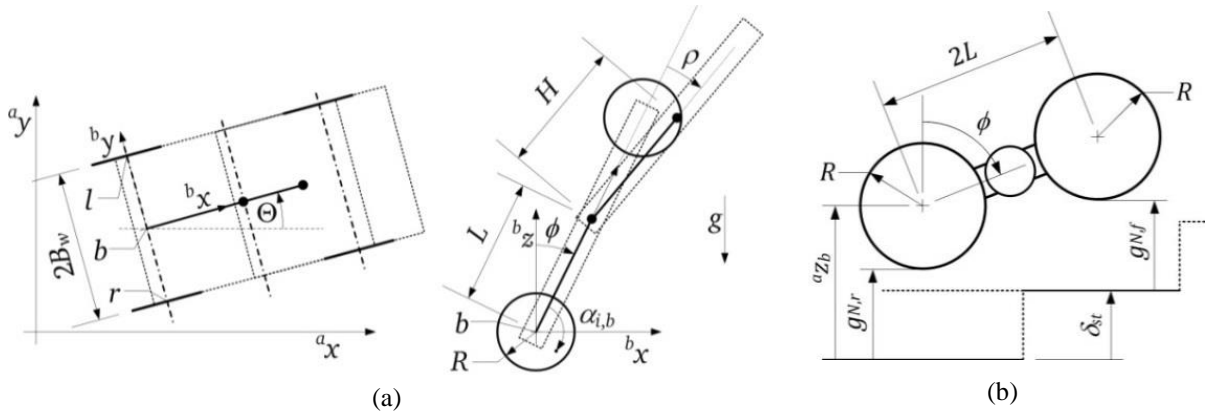


Figure 5: (a) The SC geometry model, (b) Geometry specific values for stair-climbing.

For control design it is convenient to consider a smaller set of independent coordinates \mathbf{v}_{S_i} rather than the set of dependent coordinates \mathbf{q} . Although the set \mathbf{v}_{S_i} is different in each state S_i it is interesting to consider it only in control design relevant states S_1 and S_3 . Furthermore, it is more convenient to consider longitudinal position l and yawing angle Θ than Cartesian position coordinates and wheel rotation angles. A relation of both sets of coordinates was done in [24] and can be stated on velocity level as:

$$\dot{\mathbf{q}} = \mathbf{J}_{\mathbf{v},S_i} \dot{\mathbf{v}}_{S_i}. \quad (7)$$

According relation matrix $\mathbf{J}_{\mathbf{v},S_1}$ and independent coordinate vector \mathbf{v}_{S_1} for the state S_1 are given in (8):

$$\mathbf{J}_{\mathbf{v},S_1} = \begin{bmatrix} \cos \Theta & 0 & 0 & 0 \\ \sin \Theta & 0 & 0 & 0 \\ 0 & 0 & 0 & 0 \\ \frac{1}{R} & -1 & 0 & -\frac{B_w}{R} \\ \frac{1}{R} & -1 & 0 & \frac{B_w}{R} \\ 0 & 1 & 0 & 0 \\ 0 & 0 & 1 & 0 \end{bmatrix}, \quad \dot{\mathbf{v}}_{S_1} = \begin{bmatrix} \dot{l} \\ \dot{\phi} \\ \dot{\rho} \\ \dot{\Theta} \end{bmatrix}. \quad (8)$$

Because the inclination angle is fixed in S_3 , the independent coordinates does not contain inclination velocity, $\dot{\mathbf{v}}_{S_3} = [\dot{l} \ \dot{\rho} \ \dot{\Theta}]^T$ and the relation matrix $\mathbf{J}_{\mathbf{v},S_3}$ equals $\mathbf{J}_{\mathbf{v},S_1}$ without second column.

Variable number of independent coordinates in different states is a further specific characteristic of hybrid dynamic systems.

Continuing the procedure using Lagrange equations of 1st kind, kinetic and potential energy of main mechanical parts was taken into account [24]. Furthermore, it was considered, that external torques were produced with current controlled DC-motors. Finally, the continuous-time model follows as differential-algebraic system:

$$\mathbf{H}_{qm}(\mathbf{q})\ddot{\mathbf{q}} + \mathbf{C}_{qm}(\mathbf{q}, \dot{\mathbf{q}}) + \mathbf{G}_q(\mathbf{q}) = \mathbf{E}_{qm} \mathbf{i}_a + \Phi_{q,S_i}^T(\mathbf{q}) \lambda_{S_i}, \quad (9)$$

$$\Phi_{q,S_i}(\mathbf{q})\ddot{\mathbf{q}} + \dot{\Phi}_{q,S_i}(\mathbf{q})\dot{\mathbf{q}} = \mathbf{0}. \quad (10)$$

Equations components of system inertia matrix $\mathbf{H}_{qm} \in \mathbb{R}^{7 \times 7}$, Coriolis and centrifugal vector $\mathbf{C}_{qm} \in \mathbb{R}^7$, gravitational vector $\mathbf{G}_q \in \mathbb{R}^7$ and external torques matrix $\mathbf{E}_{qm} \in \mathbb{R}^{7 \times 3}$ does not vary with changing state S_i . Varying with discrete states is the constraint situation which is reflected in changing matrix Φ_{q,S_i} and constraint forces $\Phi_{q,S_i}^T(\mathbf{q}) \lambda_{S_i}$. The system can be influenced from extern via DC-motor currents $\mathbf{i}_a = [i_l, i_r, i_{body}]^T$ whereat the elements i_l , i_r and i_{body} relate to left wheel drive, right wheel drive and composed upper body drives respectively.

Considering new development of the SC_2 , additional DOF regarding payload manipulation along upper body would increase both the independent coordinates \mathbf{q} and minimal coordinates \mathbf{v}_{S_i} by three. Equivalently, additional system inputs in \mathbf{i}_a are necessary for payload manipulation.

3.3 Discontinuous dynamics

In opposite to continuous-time dynamics some of system changes, like wheel-to-ground contact activation and deactivation are of discontinuous nature. These events correspond to the process of discrete state transitions, *settling* and *lift-off*. Contact dynamics described here correspond to exemplarily description in chapter 3.1. Details of multiple contact specifics are given in [24] [25].

Geometry relevant values considering the process of *settling* are depicted on Figure 5-b. Essential for contact activations are wheel-to-ground normal direction distances $g_{N,f}$ and

$g_{N,r}$ of the front and rear wheel pair respectively (indices denotation: N – normal direction, f – front, r – rear), whereat δ_{St} represents the step height:

$$\begin{aligned} g_{N,r} &= {}^a z_b - R, \\ g_{N,f} &= {}^a z_b + 2L \cos \phi - R - \delta_{St}. \end{aligned} \quad (11)$$

The guard functions described on logical level in chapter 3.1 can now be specified in detail. An indication $J_{A,f} \in \{\text{true}, \text{false}\}$ of impact and potential entrance to next state is defined with zero distance and negative velocity (index A denotes – immediately before impact, index E denotes – immediately after impact):

$$J_{A,f} := g_{NA,f} = 0 \wedge \dot{g}_{NA,f} < 0. \quad (12)$$

In the case that the rebound velocity after impact is bigger than zero, the impact indication $J_{E,f} \in \{\text{true}, \text{false}\}$ of this event is defined as

$$J_{E,f} := \dot{g}_{NE,f} > 0. \quad (13)$$

Oppositely, if the velocity after impact is zero, the contact indication $C_{A,rf} \in \{\text{true}, \text{false}\}$ is expressed with

$$C_{A,rf} := \dot{g}_{NE,r} = 0 \wedge \dot{g}_{NE,f} = 0. \quad (14)$$

Considering general situation of both normal coordinates $\mathbf{g} = [g_{N,r}, g_{N,f}]^T$ and all states S_i , the impact is modeled as Newton's impact with ϵ_N as restitution factor and $\dot{\mathbf{g}}_{NA,S_i}$ and $\dot{\mathbf{g}}_{NE,S_i}$ as normal direction velocities before and after impact respectively:

$$\dot{\mathbf{g}}_{NE,S_i} = -\epsilon_N \dot{\mathbf{g}}_{NA,S_i} \quad (15)$$

The connection of the normal direction velocity to general coordinate velocity is given with constraint matrix:

$$\dot{\mathbf{g}}_{NA,S_i} = \Phi_{\mathbf{q},S_i} \dot{\mathbf{q}}_A. \quad (16)$$

Impact impulses Λ_{N,S_i} can be calculated from both velocities using (9) on impulse level:

$$\Lambda_{N,S_i} = (\Phi_{\mathbf{q},S_i} \mathbf{H}_{\mathbf{q}}(\mathbf{q}_A)^{-1} \Phi_{\mathbf{q},S_i}^T)^{-1} (\dot{\mathbf{g}}_{NE,S_i} - \dot{\mathbf{g}}_{NA,S_i}). \quad (17)$$

Now the system velocities can be determined:

$$\dot{\mathbf{q}}_E = \dot{\mathbf{q}}_A + \mathbf{H}_{\mathbf{q}}(\mathbf{q}_A)^{-1} \Phi_{\mathbf{q},S_i}^T \Lambda_{N,S_i}. \quad (18)$$

Equation (18) defines the reset functions $\mathcal{R}_{1 \rightarrow 3}$ and $\mathcal{R}_{1 \rightarrow 1}$. The sudden value change of the continuous state vector \mathbf{q} due to impulse change is a further typical characteristic of hybrid dynamic systems.

Allowing *lift-off*, the contact deactivation represents a further possible event. Contact deactivation is detected by disappearing of particular wheel-to-ground forces. Considering exemplarily description of *lift-off* with front wheels (1), corresponding front wheel-to-ground force λ_f disappearance is defined with:

$$C_{E,f} := \lambda_f = 0 \wedge \dot{\lambda}_f < 0. \quad (19)$$

There is no velocity change with contact deactivation. Hence, appropriate reset function $\mathcal{R}_{3 \rightarrow 1}$ can be omitted meaning that $\dot{\mathbf{q}}_E = \dot{\mathbf{q}}_A$.

3.4 Model in minimal coordinates

For a consideration in a particular discrete state S_i it is convenient to consider only the smaller independent set of coordinates in a simplified model, even if the constraint force information is not present anymore. A use case for this model is control design in particular states. Since only states S_1 and S_3 are relevant for control design, these states correspond the consideration in the following.

The model in minimal number of coordinates follows after derivation considering relation (7) on velocity and acceleration level:

$$\mathbf{H}_{\mathbf{v}_{S_i}}(\mathbf{v}_{S_i}) \dot{\mathbf{v}}_{S_i} + \mathbf{C}_{\mathbf{v}_{S_i}}(\mathbf{v}_{S_i}, \dot{\mathbf{v}}_{S_i}) = \mathbf{E}_{\mathbf{v}_{S_i}} \mathbf{i}_{\mathbf{v}}, \quad i \in \{1,3\} \quad (20)$$

where $\{\mathbf{H}_{\mathbf{v}_{S_1}} \in \mathbb{R}^{4 \times 4}, \mathbf{H}_{\mathbf{v}_{S_3}} \in \mathbb{R}^{3 \times 3}\}$ and $\{\mathbf{C}_{\mathbf{v}_{S_1}} \in \mathbb{R}^4, \mathbf{C}_{\mathbf{v}_{S_3}} \in \mathbb{R}^3\}$ represent inertia matrices and velocity/position depended matrices respectively. Matrices $\{\mathbf{E}_{\mathbf{v}_{S_1}} \in \mathbb{R}^{4 \times 3}, \mathbf{E}_{\mathbf{v}_{S_3}} \in \mathbb{R}^{3 \times 3}\}$ assign particular system inputs of $\mathbf{i}_{\mathbf{v}} = [i_{long}, i_{body}, i_{yaw}]^T$ to the corresponding \mathbf{v}_{S_i} coordinate. These inputs are motor currents proportional to motor torques, whereat the input $i_{long} = i_r + i_l$ builds the longitudinal direction motor current and $i_{yaw} = i_r - i_l$ represent the yawing motor current.

3.5 Equilibrium points

Equilibrium points for both control relevant discrete states can be derived from model (20) at stationery state [24].

Considering S_1 , depending on the inclination angle ϕ_0 , a body torque generated by body drive current i_{body} holds the robot upright in equilibrium with a definite relative body angle ρ_0 . The relation between two mentioned angles is continuous and follows as:

$$\rho_0 = f_{bal}(\phi_0) = \arcsin\left(\frac{-L(M_B + 4m_{wd} + M)\sin(\phi_0)}{HM_B}\right) - \phi_0 \quad (21)$$

whereat parameters are: upper body mass $M_B = 16$ kg, lower body mass $M = 3.3$ kg and front wheel mass $m_{wd} = 0.4$ kg.

The function is depicted in Figure 6-a showing relevant inclination angle range. Figure 6-b shows exemplarily three possible SC equilibrium configurations.

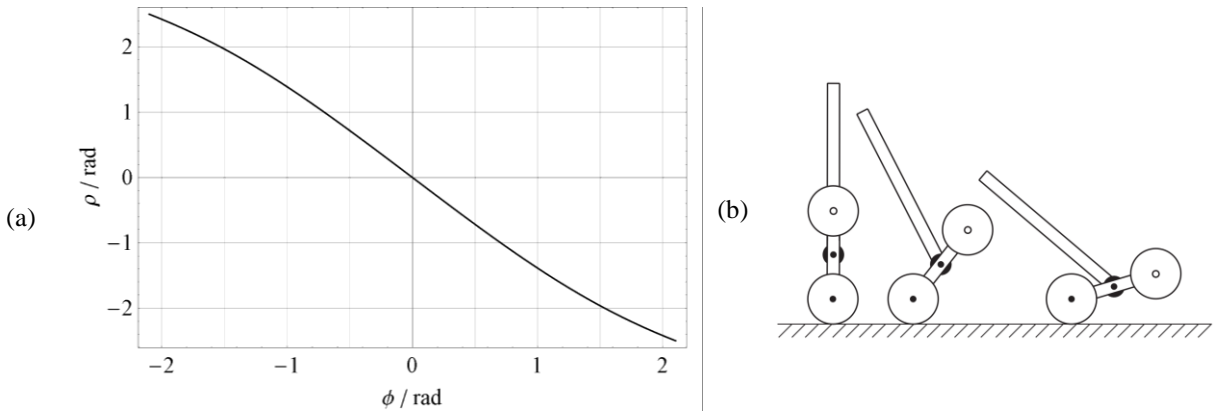


Figure 6: (a) Angle configuration in equilibrium, (b) Three possible SC equilibrium configurations.

Considering S_3 , possible are variable relative body angles ρ in a certain range while the

inclination angle ϕ is fixed with ground.

Considering new development of the SC_2 , the stationary equilibrium function would depend also on the additional DOFs.

3.6 Simulation

The simulation of the robot hybrid dynamic system represented with hybrid automaton on Figure 4 gives insight in overall system behavior.

Since it consists of interacted continuous-time and discontinuous dynamics, this paradigm was followed in implementation within Matlab for simulation and is schematically shown in Figure 7.

The continuous-time dynamics is represented with the differential-algebraic system (9)-(10). Using symbolic solvers like Mathematica there is a possibility to receive explicit analytical solution consisting of the acceleration $\ddot{\mathbf{q}}$ and Lagrange multiplier λ_{S_i} . Since this solution is too bulky to achieve simulation results in meaningful simulation time, the system was solved numerically within Simulink in each simulation step. Influenced from outside by the input \mathbf{i}_a the solution provides position/velocity information $[\mathbf{q}, \dot{\mathbf{q}}]^T$, distance to ground of both wheel pairs $[g_{N,r}, g_{N,f}]^T$ and wheel-to-ground normal forces $[\lambda_r, \lambda_f]^T$. The last two information sets are used to detect events like impacts and lift-offs respectively.

The discontinuous dynamics is event driven. Detection of those, like wheel-to-ground impact or wheel-to-ground force disappearance is described in chapter 3.3. Under influence of this events, depending on current discrete state S_j state transitions $S_j \rightarrow S_i$ evolve regarding rules described in chapter 3.1. The discontinuous dynamics was implemented within a state-machine in Stateflow. The outputs consisting of discontinuously changed positions/velocities together with a reset signal and new state information S_i are fed back into the continuous-time part.

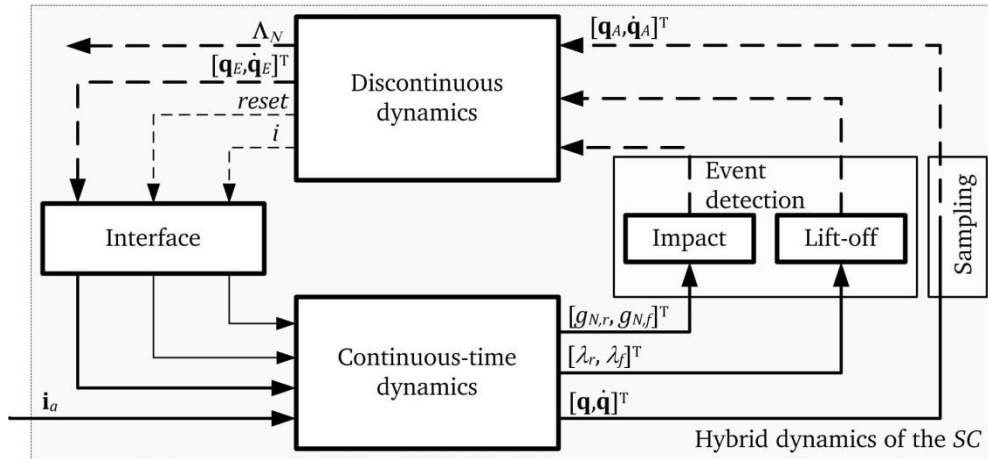


Figure 7: Implementation scheme of the SC for simulation in Matlab.

Critical for simulation results plausibility is the event detection. The event detection was implemented in Simulink using zero-crossing detection within the ‘Hit Crossing’ block. After a sign change of the observed quantity, the zero-crossing algorithm starts to search for the precise zero-crossing time. This implies the using of variable-time solvers for simulation. To increase the precision, the zero-crossing algorithm within Simulink was set to ‘Adaptive’. Different simulation time and scenario plausibility outcomes were achieved by using

different solver types [24]. Furthermore, due to system intrinsic *Zeno*-behavior, the contact indication allowing state transitions is relaxed, e.g. in (14) there is a change to $|\dot{g}_{NE,f}| \leq \varepsilon$, $\varepsilon \in \mathbb{R}^+$ allowing small positive value ε instead of zero.

4 CONTROL

Specific for the control task definition for this robot is the intrinsic hybrid nature during the stair-climbing. Therefore, the task definition should consider not only control within the continuous space of a particular discrete state S_i but also the state transitions of the discrete states.

The model-based control design methods are related to feedback linearization, considering the nonlinear system characteristics in a particular discrete state. Since the methods rely on use of all system state variables, not measurable variables are estimated. In following subchapters the estimation principle is described before the relevant control design methods.

Considering new development of the SC_2 , the additional actuated DOF gives more flexibility in control design of both topics – in equilibrium points and state transitions.

4.1 Inclination angle determination

The inclination angle is a system state variable needed in the feedback for the control design implementation but not measurable with sufficient performance. In opposite, other system state variables are either directly measurable or achievable through simple kinematic relations.

The inclination angle determination is based on a sensor data fusion of two sensors implemented within an observer structure. The principle is described in detail in [24] [26] and adapted to case of this robot.

Data of two sensors, an inclinometer and a gyroscope is used to extract their beneficial properties in particular dynamic ranges. The inclinometer provides sufficient stationary accuracy and the gyroscope provides dynamic content.

As outcome, a high-dynamics fusion inclination angle cleaned from drift is achieved and used for control feedback.

4.2 Control structure

The overall control structure is given in [24] fulfilling all relevant control tasks. The high-level control algorithm is consisting of a sensor signal processing module which contains the sensor data fusion algorithm as well as sensor to system state-variable coordinate transformation. Furthermore, the continuous-time functions contain continuous-time controllers involving continuous variables and set-value generation. The event-based dynamics is implemented within a state machine, whereat based on detected events and current system state the control system determines the activation of particular continuous-time controllers and triggering of the set-value generation and safety relevant functions.

The controlled system representing the robot was brought from (20) into the state space form:

$$\begin{aligned} \dot{\mathbf{x}}_{S_i} &= \mathbf{f}_{S_i}(\mathbf{x}_{S_i}) + \mathbf{g}_{S_i}(\mathbf{x}_{S_i})\mathbf{i}_v, \\ \mathbf{y}_{S_i} &= \mathbf{h}_{S_i}(\mathbf{v}_{S_i}), \end{aligned} \quad i \in \{1,3\}, \quad (22)$$

whereat the smooth vector fields for both considered states $\{\mathbf{f}_{S_1} \in \mathbb{R}^{8 \times 1}, \mathbf{f}_{S_3} \in \mathbb{R}^{6 \times 1}\}$, $\{\mathbf{g}_{S_1} \in \mathbb{R}^{8 \times 3}, \mathbf{g}_{S_3} \in \mathbb{R}^{6 \times 3}\}$ and $\{\mathbf{h}_{S_1} \in \mathbb{R}^{3 \times 1}, \mathbf{h}_{S_3} \in \mathbb{R}^{3 \times 1}\}$ represents the system, the input

and the output functions respectively. The minimal coordinates and according velocities form the state space vector $\mathbf{x}_{S_i} = [\mathbf{v}_{S_i}^T, \dot{\mathbf{v}}_{S_i}^T]^T$.

With appropriate switching within the control structure, it is possible to apply tracking control in both considered states S_1 and S_3 and control of both state transitions $S_1 \rightarrow S_3$ and $S_3 \rightarrow S_1$.

4.3 Control in equilibrium points

Tracking control tasks in both considered states S_1 and S_3 relate to motion along equilibrium points described in chapter 3.5. Feedback linearization method allows linearization in the whole operating range. The system (22) analysis gives the system order of 8 and 6 in states S_1 and S_3 respectively. Corresponding vector relative degree is determined to $r = \{2,2,2\}$.

The controlled variables in both states are the position l , the upper body angle ρ and the yaw angle θ . This determines the output function $\mathbf{y}_{S_i} = [l, \rho, \theta]^T$.

While in the state S_3 the system is fully actuated resulting in full relative degree and input-state feedback linearization, the situation in S_1 more complex. The system is under-actuated in S_1 due to additional coordinate ϕ while additional actuator is not present. This corresponds to mismatch of the system order and sum of r . Consequently, only a partial (input-output) feedback linearization is possible, leaving a part of the system nonlinear. This nonlinear part corresponding to dynamics of the inclination angle ϕ represents the internal dynamics, not visible in the system output. Nevertheless, since their analysis shows equilibrium instability, it has to be taken into account for control design.

Therefore, in case of S_1 all system variables are taken into account for stabilization using a LQ control while in case of S_3 stabilization was done using multichannel PD control.

Considering new development of the SC_2 , the additional actuated DOFs would increase the number of input-output channels but the particular relative degree would stay 2. Considering stabilization with a fixed longitudinal position l , which is beneficial on stair, additional DOFs allow e.g. use of payload manipulation. This can be advantageous since upper body ρ and longitudinal position l can be relieved of manipulation.

4.4 Control of state transitions

In opposite to control in equilibrium points, the control of state transitions considers system motion between equilibrium points. Theoretical consideration within Chapter 4.4 regards to state transitions on flat ground, which differ to case of stair in step height $\delta_{St} \neq 0$.

Conditions for state transitions were analyzed in [24] [27] before control design. Since stair-climbing is assumed to proceed in confined space, state transitions are performed mainly due to motion of upper body angle ρ while longitudinal position l and yawing angle θ are held constant.

Obviously, the condition for *settling* ($S_1 \rightarrow S_3$) is that the lower body has to touch the ground with zero touchdown velocity. In case of flat ground it implies $\phi = \pi/2 \wedge \dot{\phi} = 0$.

The condition for *lift-off* ($S_3 \rightarrow S_1$) is that the front wheel-to-ground contact force depending on upper body kinematics disappears getting into space $\lambda_f(\rho, \dot{\rho}, \ddot{\rho}) < 0$. This condition was visualized as blue space in Figure 8. Similarly, a red space represents the condition of *lift-off* with rear wheels $\lambda_r(\rho, \dot{\rho}, \ddot{\rho}) < 0$.

While conditions for state transitions are explicit, strategies involving additional criterion are ambiguous.

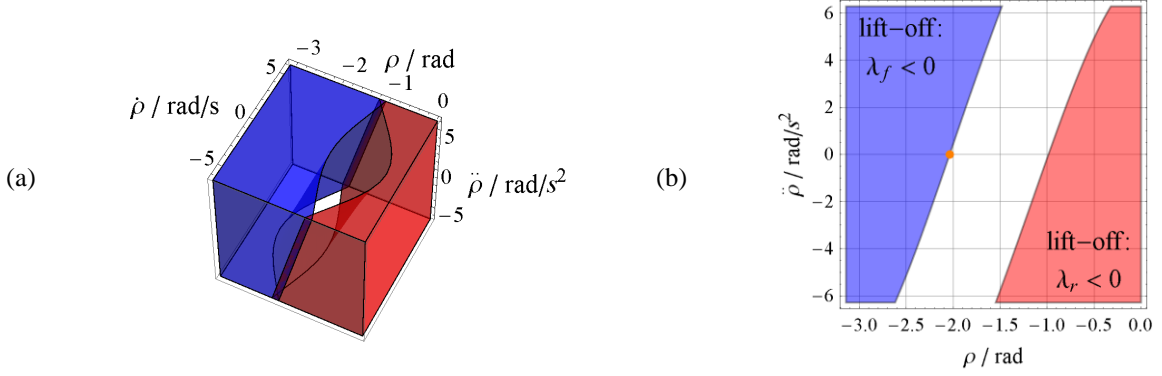


Figure 8: Condition space for *lift-off* depending on the upper body kinematics: (a) the complete space, (b) cross-section at $\dot{\rho} = 0$. Critical point representing the border between states S_1 and S_3 in equilibrium (orange dot).

The strategy for *lift-off* ($S_3 \rightarrow S_1$) was implemented using appropriate tracking control in S_3 by a motion of the upper body whereat the same time other coordinates are held zero. Additional considered condition is slipping prevention of the rear wheels [25]. After reaching state S_1 , the control was switched to stabilization to preserve the equilibrium.

The strategy for *settling* ($S_1 \rightarrow S_3$) was found allowing stable and theoretically bump-free touch-down [24] [27]. Starting from equilibrium in S_1 this was achieved by initiating the robot falling to ground into wanted direction. As soon as the inclination angle is approaching ground, appropriate actuated upper body motion produces a reaction torque on the lower body causing deceleration. Finally, the touch-down is ideally bump-free. After contact, the upper body only needs to be decelerated to standstill.

The *settling* strategy was implemented within virtual constraints framework [18] where the output functions are only dependent on the position \mathbf{v}_{S_i} . The consideration regards S_1 , where the system is under-actuated. To move the upper body depending on the inclination angle ϕ , a function $f_{S_\tau}(\phi)$ is established to the system output function:

$$\mathbf{y}_{S_\tau} = \mathbf{h}_{S_\tau}(\mathbf{v}_{S_1}) = \begin{bmatrix} l \\ \rho - f_{S_\tau}(\phi) \\ \Theta \end{bmatrix}. \quad (23)$$

Following the control design procedure [20], a valid coordinate transformation Ψ_{S_τ} results in a separation of the external dynamics coordinates ξ_{S_τ} and internal dynamics coordinates η :

$$\mathbf{z}_{S_\tau} = \Psi_{S_\tau}(\mathbf{x}_{S_1}) = \begin{bmatrix} l \\ \dot{l} \\ \rho - f_{S_\tau}(\phi) \\ \dot{\rho} - f'_{S_\tau}(\phi)\dot{\phi} \\ \Theta \\ \dot{\Theta} \\ \text{---} \\ \phi \\ \dot{\phi} \end{bmatrix} = \begin{bmatrix} \xi_{S_\tau} \\ \eta \end{bmatrix}. \quad (24)$$

Corresponding feedback $\mathbf{r}_{S_\tau} = \mathbf{R}_{A,S_\tau}^{-1} \mathbf{R}_{b,S_\tau}$ and feed-forward $\mathbf{v}_{S_\tau} = \mathbf{R}_{A,S_\tau}^{-1}$ term provide the linearization of the external system dynamics leaving the internal dynamics still nonlinear:

$$\begin{aligned}
 \dot{\xi}_{S_\tau} &= \mathbf{A}_{f_l, S_\tau} \xi_{S_\tau} + \mathbf{B}_{f_l, S_\tau} \mathbf{v} \\
 \dot{\eta}(\xi_{S_\tau}, \boldsymbol{\eta}) &= \mathbf{w}(\xi_{S_\tau}, \boldsymbol{\eta}) + \mathbf{t}(\xi_{S_\tau}, \boldsymbol{\eta}) \mathbf{R}_{A, S_\tau}^{-1}(\xi_{S_\tau}, \boldsymbol{\eta}) (\mathbf{v} - \mathbf{R}_{b, S_\tau}(\xi_{S_\tau}, \boldsymbol{\eta})) \\
 \mathbf{y}_{S_\tau} &= \mathbf{C}_{f_l, S_\tau} \xi_{S_\tau}
 \end{aligned} \quad (25)$$

The partly linearized system is now driven by new control input \mathbf{v} . The external dynamics involving ξ_{S_τ} consists of three double integrators corresponding to the coordinate channels l , ρ and Θ . They are defined by system, input and output matrices \mathbf{A}_{f_l, S_τ} , \mathbf{B}_{f_l, S_τ} , and \mathbf{C}_{f_l, S_τ} respectively. Corresponding to particular coordinate channels, three PD-controllers stabilize the external dynamics of the system and zeroes asymptotically the state variable ξ_{S_τ} . Consequently, the virtual constraint takes strength, $\rho \rightarrow f_{S_\tau}(\phi)$ and the internal dynamics comes to his nominal zero dynamics:

$$\dot{\eta}(\mathbf{0}, \boldsymbol{\eta}) = \begin{bmatrix} \dot{\phi} \\ f_{\eta, 2}(\boldsymbol{\eta}) \end{bmatrix}. \quad (26)$$

The zero dynamics (26) is a 2nd order nonlinear differential equation describing the designed dynamics of the inclination angle ϕ . The function $f_{\eta, 2}(\boldsymbol{\eta})$ includes the system mechanical elements of $\mathbf{H}_{v_{S_i}}$ and $\mathbf{C}_{v_{S_1}}$ and the virtual constraint function $f_{S_\tau}(\phi)$ derivatives. Hence, the introduced function $\rho = f_{S_\tau}(\phi)$ has a crucial influence on zero dynamics, and was designed ([24], Figure 9-a) to meet the *settling* strategy described before.

Figure 9-b shows that after *settling* start, as soon as the ground comes near (touch-down angle $\phi_{TD} = \pi/2$) due to acceleration of the upper body ρ the inclination angle velocity slows down. Thereby, the critical point which would not lead to stable transition [27] is avoided. Finally, the ground is reached with significantly decreased velocity comparing to case of falling with fixed upper body. The nominal zero dynamics trajectory $\boldsymbol{\eta}_0^*$ shows local stability [24] [27]. The touch-down velocity ($\dot{\phi}_{TD}$ at $\phi_{TD} = \pi/2$) is not ideally zero allowing certain robustness against real system uncertainty [24].

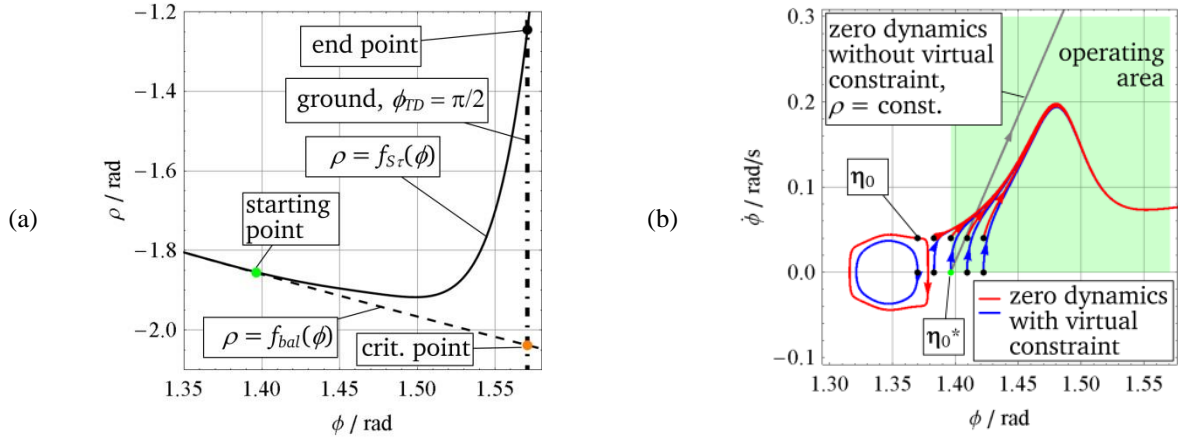


Figure 9: (a) Virtual constraint $\rho = f_{S_\tau}(\phi)$ and (b) corresponding zero dynamics phase portrait. Gray trajectory is added for comparison representing fixed upper body angle ρ during falling.

Considering new development of the SC_2 , the additional payload DOFs can be included into control design of the state transitions. For instance, during *settling* there is the possibility to induce reaction torque on lower body through payload manipulation. Together with upper body manipulation this allows more freedom for optimization of the motion trajectory. For

instance, amplitude changes of upper body ρ can be decreased due to payload manipulation.

5 RESULTS

The stair-climbing procedure is presented as a collected sequence of particular motion scenarios on video [28]. It consists of scenarios like *lift-off* and *settling* on ground, and later on stair. A part of the stair-climbing procedure is rotation of the lower body shown also in Figure 10.

In continuation of this motion, *settling* on a stair is chosen here for more detailed presentation (Figure 11) as a motion scenario with most control design effort. This motion is realized based on method described in chapter 4.4. The virtual constraint applied for *settling* on Figure 11 was adapted to the case of considered step but it is qualitatively the same as the one used in chapter 4.4.

The measurement in Figure 11 starts with Balancing in S_1 (for $t < 0$). The falling is initiated with switching to *settling* transition at $t = 0$. According to implemented virtual constraint, as soon as the lower body approaches ground, the upper body accelerates causing reaction torque on lower body. This torque slows the lower body down, reaching the ground with low zero normal direction velocity. Hence, the touch-down is smooth and afterwards only the upper body is decelerated to zero.

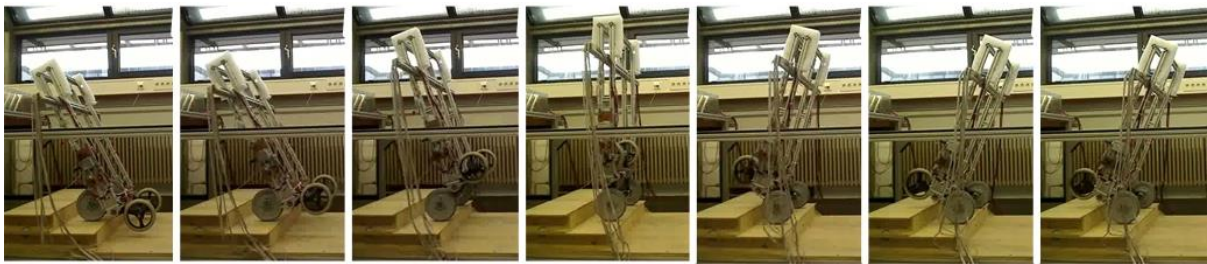


Figure 10: Rotation of the *SC* lower body as a part of the stair-climbing procedure (snapshot every 2.29 s).

In parallel with measurement, a simulation is given for comparison starting with falling at $t = 0$. The behavior of *settling* corresponds qualitatively to measurement with some deviations. Due to not considered Coulomb friction in model, the falling initiation at $t = 0$ exhibits larger amplitude changes visible at velocities. For same reason, additional motion activity is visible at $t \approx 0.9 \text{ s} \div 1.1 \text{ s}$ in measurement, where the upper body change his motion direction passing through $\dot{\rho}_m = 0$ with a break. Further deviations are present due to additional sensor data fusion in measurement, higher frequency modes of the real system, noise, quantization, wheel elasticity of the real wheels, hanging cables etc. Nevertheless, *settling* transition proceeds stably showing a certain amount of robustness due to mentioned differences between real system and model.

Further motion scenarios are available in [24], [25] and [27].

6 CONCLUSION AND OUTLOOK

The autonomous stair-climbing with the wheel-based robot *SC* was achieved as a stable and repeatable motion sequence.

The hybrid dynamic model of the *SC* covers the minimum number of discrete states allowing control design strategy. The continuous-time dynamics allows model-based control concepts developed for nonlinear systems, although it could be extended with some real system phenomenon like Coulomb friction or wheel elasticity.

Both, control in equilibrium points and control of state transitions were successfully realized. Nevertheless, they offer potentials for optimization and enhancements. Together with consideration of additional DOFs, alternatives for control could give more optimization possibility regarding amplitude magnitude of particular DOFs, operational range validity and dynamics intensity. An alternative control paradigm, stable limit cycles can be examined to provide more energy-efficient and robust locomotion. It should provide a permanent lower body rotation during stair-climbing instead of a sequence of motion of current robot.

Finally, to stress out further application advantages of the robot locomotion type presented here, in balancing state on one wheel pair it has a tall and slim contour, which makes it applicable in narrow spaces. To be handy, a certain robot height is necessary since human are in focus for this application. Generally, movability benefits from an active control stabilization since the wheelbase can be built shorter. Consideration of additional DOFs could improve comfort, flexibility to different stair geometry and dynamic behavior.

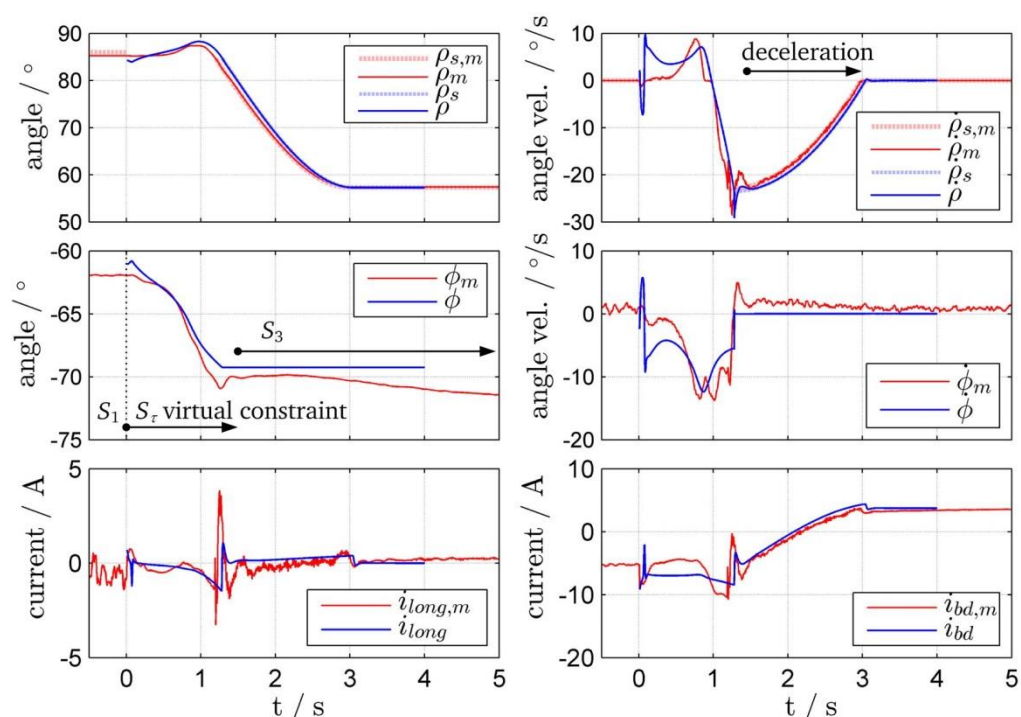


Figure 11: State transition *settling* in a stair case, measurement (add. index m) vs. simulation (w/o add. index). Additional index s denotes set value.

REFERENCES

- [1] B. Strah und S. Rinderknecht, „Stair-Climbing Assistive Robots (The Impact of Control Technology—2nd Ed.),“ [Online]. Available: <http://ieeecss.org/sites/ieeecss.org/files/CSSIoCT2Update/IOCT2-RC-Strah-1.pdf>. [Access on 13 April 2015].
- [2] B. Siciliano und O. Khatib, Handbook of Robotics, Berlin, Heidelberg: Springer-Verlag, 2008.

- [3] O. Matsumoto, S. Kajita, M. Saigo und K. Tani, „Dynamic trajectory control of passing over stairs by a biped type leg-wheeled robot with nominal reference of static gait,“ in Conference on Intelligent Robots and Systems, 1998. Proceedings., 1998 IEEE/RSJ International, Victoria, BC, Canada, 1998.
- [4] K. Hashimoto, T. Hosobata, Y. Sugahara, Y. Mikuriya, H. Sunazuka, M. Kawase, H.-o. Lim und A. Takanishi, „Realization by Biped Leg-wheeled Robot of Biped Walking and Wheel-driven Locomotion,“ in Conference on Robotics and Automation, 2005. ICRA 2005. Proceedings of the 2005 IEEE International, 2005.
- [5] Wikipedia, „iBOT,“ [Online]. Available: <http://en.wikipedia.org/wiki/IBOT>. [Access on 13 April 2015].
- [6] M. J. Lawn, Study of stair-climbing assistive mechanisms for the disabled, Nagasaki: Dissertation at Nagasaki University, 2002.
- [7] O. Matsumoto, S. Kajita, K. Tani und M. Ooto, „A four-wheeled robot to pass over steps by changing running control modes,“ in Conference on Robotics and Automation, 1995. Proceedings., 1995 IEEE International, Nagoya, 1995.
- [8] O. Matsumoto, S. Kajita und K. Tani, „Dynamic trajectory control of a variable structure type four-wheeled robot to pass over steps,“ in International Workshop on Advanced Motion Control, 1996. AMC '96-MIE. Proceedings., 1996 4th, Mie, 1996.
- [9] O. Matsumoto, S. Kajita und K. Tani, „Fast passing over steps with unknown height by a 'variable structure type four-wheeled robot',“ in Conference on Intelligent Robots and Systems, 1997. IROS '97., Proceedings of the 1997 IEEE/RSJ International, Grenoble , 1997.
- [10] O. Matsumoto, S. Kajita und K. Komoriya, „Flexible locomotion control of a self-contained biped leg-wheeled system,“ in Conference on Intelligent Robots and Systems, 2002. IEEE/RSJ International, Ibaraki, Japan, 2002.
- [11] A. v. d. Schaft und H. Schumacher, An introduction to hybrid dynamical systems, London: Springer-Verlag, 2000.
- [12] J. Lunze und F. Lamnabhi-Lagarrigue, Handbook of Hybrid Systems Control - Theory, Tools, Applications, Cambridge CB2 8RU, UK: Cambridge University Press, 2009.
- [13] F. Pfeiffer und C. Glocker, Multibody Dynamics with Unilateral Contacts, New York: John Wiley & Sons, Inc., 1996.
- [14] F. Pfeiffer, Mechanical System Dynamics, Berlin, Heidelberg: Springer-Verlag, 2008.
- [15] C. Studer und C. Glocker, „Simulation of Non-smooth Mechanical Systems with many Unilateral Constraints,“ in ENOC-2005, Eindhoven. Netherlands, 2005.

- [16] R. Zander, T. Schindler, M. Friedrich, R. Huber, M. Förg und H. Ulbrich, „Non-smooth dynamics in academia and industry: recent work at TU München,“ *Acta Mechanica* 195, pp. 167-183, 2008.
- [17] V. Acary und B. Brogliato, *Numerical Methods for Nonsmooth Dynamical Systems*, Berlin: Springer-Verlag, 2008.
- [18] E. J. Westervelt, J. W. Grizzle, C. Chevallereau, J. H. Choi und B. Morris, *Feedback Control of Dynamic Bipedal Robot Locomotion*, Boca Raton: Taylor & Francis Group, 2007.
- [19] C. Canudas-de-Wit, „On the concept of virtual constraints as a tool for walking robot control and balancing,“ *Annual Reviews in Control*, Bd. 28, pp. 157-166, 2004.
- [20] A. Isidori, *Nonlinear Control Systems*, 3. Hrsg., London: Springer-Verlag, 1995.
- [21] M. M. Dalvand und B. Shirinzadeh, „Dynamic Modelling, Tracking Control and Simulation Results of a Novel Underactuated Wheeled Manipulator (WAcrobot),“ in *Advanced Strategies for Robot Manipulators*, Rijeka, Sciyo, 2010, pp. 91-106.
- [22] M. W. Spong, „The Swing Up Control Problem For The Acrobot,“ *IEEE Control Systems Magazine*, Bd. 15, Nr. 1, pp. 49-55, February 1995.
- [23] K. Lee und V. Coverstone-Carroll, „Control Algorithms for Stabilizing Underactuated Robots,“ *Journal of Robotic Systems*, pp. 681-697, 1998.
- [24] B. Strah, „Control of a wheeled double inverted pendulum considering hybrid dynamics (in German),“ 2012. [Online]. Available: <http://tuprints.ulb.tu-darmstadt.de/3050/>.
- [25] B. Strah und S. Rinderknecht, „Hybrid Dynamic Model of a Wheeled Double Inverted Pendulum,“ in *22nd Mediterranean Conference on Control & Automation*, Palermo, 2014.
- [26] B. Strah und S. Rinderknecht, „High Dynamics Tilt Estimation using Simple Observer,“ in *IEEE EuroCon*, Zagreb, 2013.
- [27] B. Strah und S. Rinderknecht, „Autonomous stair climbing of a wheeled double inverted pendulum,“ in *The 6th IFAC Symposium on Mechatronic Systems*, Hangzhou, 2013.
- [28] YouBrownful, „YouTube,“ September 2012. [Online]. Available: <http://youtu.be/3BPhm1frfk8>.